Oxidation of Metals, Vol. 23, Nos. 1/2, 1985

The Influence of Alloy Microstructure on the Oxide Peg Morphologies in a Co–10% Cr–11% Al Alloy With and Without Reactive Element Additions

R. Pendse* and J. Stringer*

Received July 10, 1984

The addition of reactive elements such as yttrium or hafnium to heat-resisting alloys has marked beneficial effects on their high-temperature oxidation behavior, and in particular greatly improves the adhesion of the oxide scale to the substrate. In the case of alloys forming Al_2O_3 protective oxide scales, the improvement in adhesion appears to be related to the formation of intrusions of oxide into the metal—"pegs"—which hold the scale on. The morphology of these pegs is a function of alloy structure and of the reactive element. In particular, it appears that while the pegs of Hf-containing alloys grow as a result of a diffusion process, perhaps along the oxide-metal phase boundary, the pegs on Y-containing alloys seem to form too fast for this, and it is suggested that stresses established by the oxidation of the Co_3Y inclusions lead to the formation of porous short-circuit paths.

KEY WORDS: scale adhesion; reactive element effect; alumina-formers; cobalt-base alloys; pegging.

INTRODUCTION

For an alloy to have good oxidation resistance at elevated temperatures, it must be able to form a protective oxide such as Cr_2O_3, Al_2O_3, or SiO_2. In addition, the protective oxide must have good adhesion to the substrate, to resist spalling on thermal cycling. It is well known that in the case of alloys forming Cr_2O_3 and Al_2O_3 scales, the addition of certain reactive elements

*Materials and Molecular Research Division, Lawrence Berkeley Laboratory, University of California, Berkeley, CA 94720.

0030-770X/85/0200-0001$04.50/0

such as yttrium or cerium greatly improves the oxide adhesion. Furthermore it has been demonstrated that fine dispersions of stable oxide particles, such as Y_2O_3, ThO_2, HfO_2, and (in the case of Cr_2O_3 formers) Al_2O_3 have a similar effect. The extensive literature on this topic has been reviewed by Whittle and Stringer.[1]

There are several theories to account for the effect of these additions on the adhesion of the scale. These include (a) the pegging model, (b) the vacancy sink model, (c) the scale plasticity model, and (d) the graded seal interface model. These models, and the evidence for and against them, are discussed in Ref. 1.

In the case of alumina formers, much of the recent work has indicated that the formation of oxide "pegs" extending into the metal is of great importance. The pegging model was introduced by Giggins and Pettit[2]; since then there have been extensive studies of the morphology of the oxide pegs formed in a number of Al_2O_3-forming alloys containing both Y and Hf as active additions.[3-6]

The morphology of pegs is plainly a factor in determining scale adhesion. Allam *et al.*[3] showed that coarse yttride particles could promote failure of the external scale. It was also shown[7] that in the Co-Cr-Al-Pt systems developed in coatings, the morphology of the Pt-containing intermetallic phases (e.g., $PtHf_3$) and their distribution in the alloy microstructure appeared to influence the oxidation behavior. In the case of vapor-deposited two-phase Co-Cr-Al coatings,[8] the Al_2O_3 oxide formed exhibited complex intrusions penetrating along the α-β boundaries, and it was speculated that these boundaries could perhaps be acting as short-circuit paths for oxygen transport.

The present study is concerned with the development of the peg morphology in a high-aluminum two-phase Co-Cr-Al alloy with and without reactive metal additions. Two reactive elements have been studied: yttrium, which has a very low solubility, and is present in the alloy as a dispersed yttride, probably having a composition close to Co_3Y;[9] and hafnium, which has a relatively high solubility and at the level studied would be expected to be in solid solution. It is believed, following Stringer *et al.*,[10] that the reactive element oxidizes in advance of the scale/metal interface to form a dispersion of oxide particles in the alloy. In the case of the yttrium-containing material, the bulk of the oxide so formed would presumably replace the yttride particles, and thus the distribution of the stable oxide particles and consequently the pegs would be determined by the yttride distribution in the alloy. In the case of the hafnium-containing alloy, since the hafnium is in solid solution, the hafnium oxide particle distribution within the alloy would presumably be a function of the various diffusion coefficients, solubility products, and the nature of the nucleation

process, and thus would be more dependent on the detailed oxidation conditions.

EXPERIMENTAL PROCEDURES

The nominal compositions of the alloys studied are shown in Table I. The alloys were prepared by induction melting from high-purity elementary metals. Ingots 50 mm diameter and 250 mm long were prepared; the stirring resulting from the induction-melting process was believed to ensure adequate homogeneity, and no further homogenization by melting or by annealing was done.

Oxidation coupons of nominal size, $10 \times 10 \times 3$ mm, were cut from these ingots and ground through 600 grit SiC paper. The specimens were then washed in soapy water and finally ultrasonically cleaned in ethyl alcohol for 5 min. The specimens were oxidized in air at temperatures between 1000°C and 1200°C for predetermined times, and weighed before and after oxidation. The specimens were contained in alumina boats to retain any scale which spalled on cooling.

After oxidation, specimens were examined metallographically, using both optical and scanning electron microscopy (SEM). Optical microscopy was performed both on cross-sections normal to the oxidation interface, and on shallow taper sections a few degrees from the plane of the interface. For the SEM studies a "deep etching" technique was used, in which the metal was dissolved away in a warm (80°C) methanol-10% bromine solution, allowing the underside of the oxide scale to be examined. The compositions of the oxide and metal phases were determined using energy dispersive X-ray analysis (EDXA) on the SEM.

RESULTS

Figure 1 shows the microstructure of the three alloys as prepared. All consist of a two-phase mixture of CoAl (dark) and Co-rich solid solution

Table I. Nominal Compositions of Alloys Studied (wt.%)

	Elements				
Alloy	Y	Hf	Al	Cr	Co
1.			11.0	10.0	Bal
2.		1.0	11.0	10.0	Bal
3.	1.0		11.0	10.0	Bal

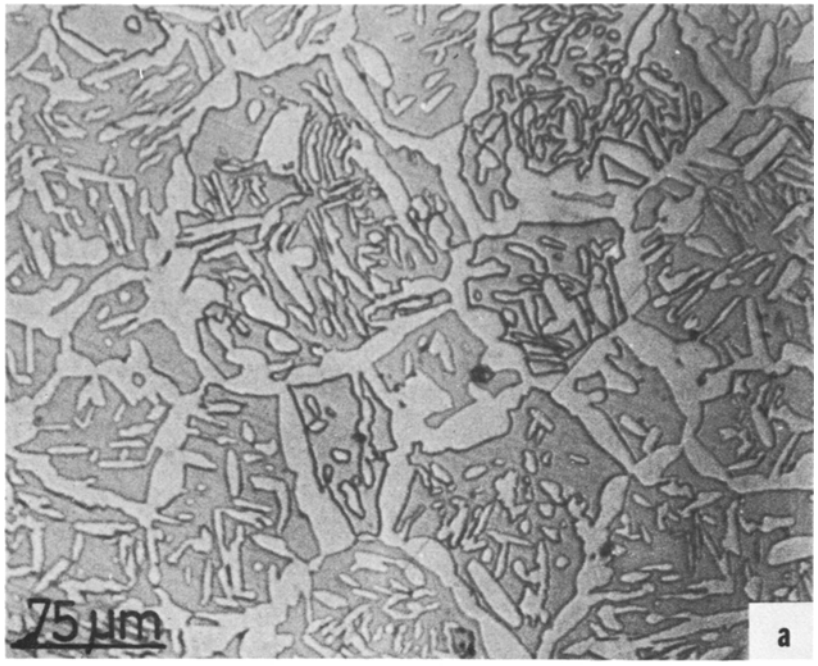
75 µm
a


75 µm
b

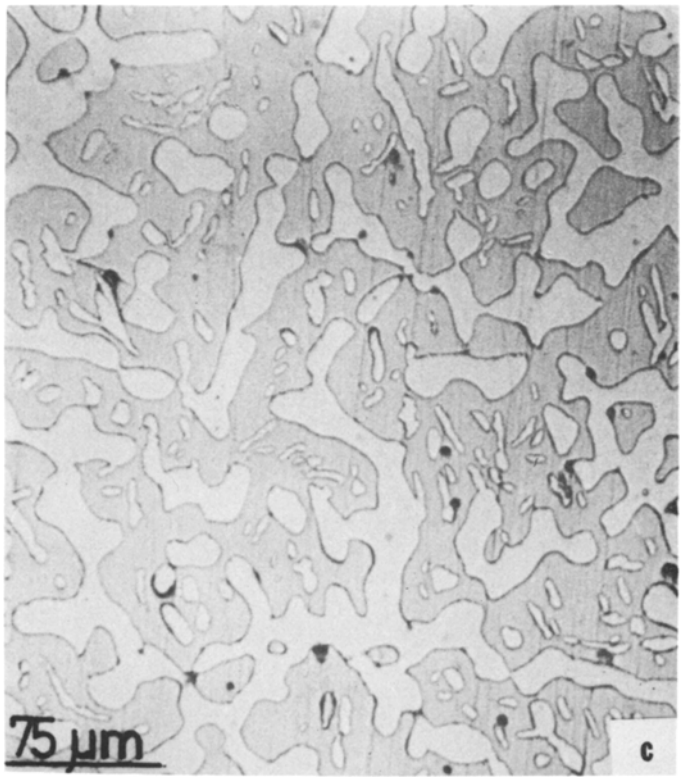

Fig. 1. Microstructures of alloys studied: (a) CoCrAl; (b) CoCrAl-Hf; (c) CoCrAl-Y.

(light). Both the yttrium and hafnium containing alloys show evidence of a third phase. Comparison with the microstructure of a Co-10Cr-11Al-0.3Y alloy shown by Allam *et al.*[3] suggests that the actual yttrium content of the alloy used in the present study may have been below the nominal 1%; in addition, the two-phase structure is much coarser for this alloy. The apparent presence of a third phase in the hafnium-containing alloy is puzzling: Allam *et al.*[3] report no third phase up to 1.5% Hf.

Figure 2 shows cross-sections of the alloys oxidized for 50 h at 1200°C. In all cases, a β-depleted layer is formed at the surface, as a result of the selective oxidation of aluminum to form an external Al_2O_3 scale. The depleted layer is approximately twice as thick in the ternary alloy as in the two alloys containing the active elements.

Depending on the average residual aluminum content in the depleted layer, the thicknes of 55 μm shown in Fig. 2a would correspond to a weight gain of about 4 mg/cm^2 and a total Al_2O_3 thickness of 22 μm. The possible

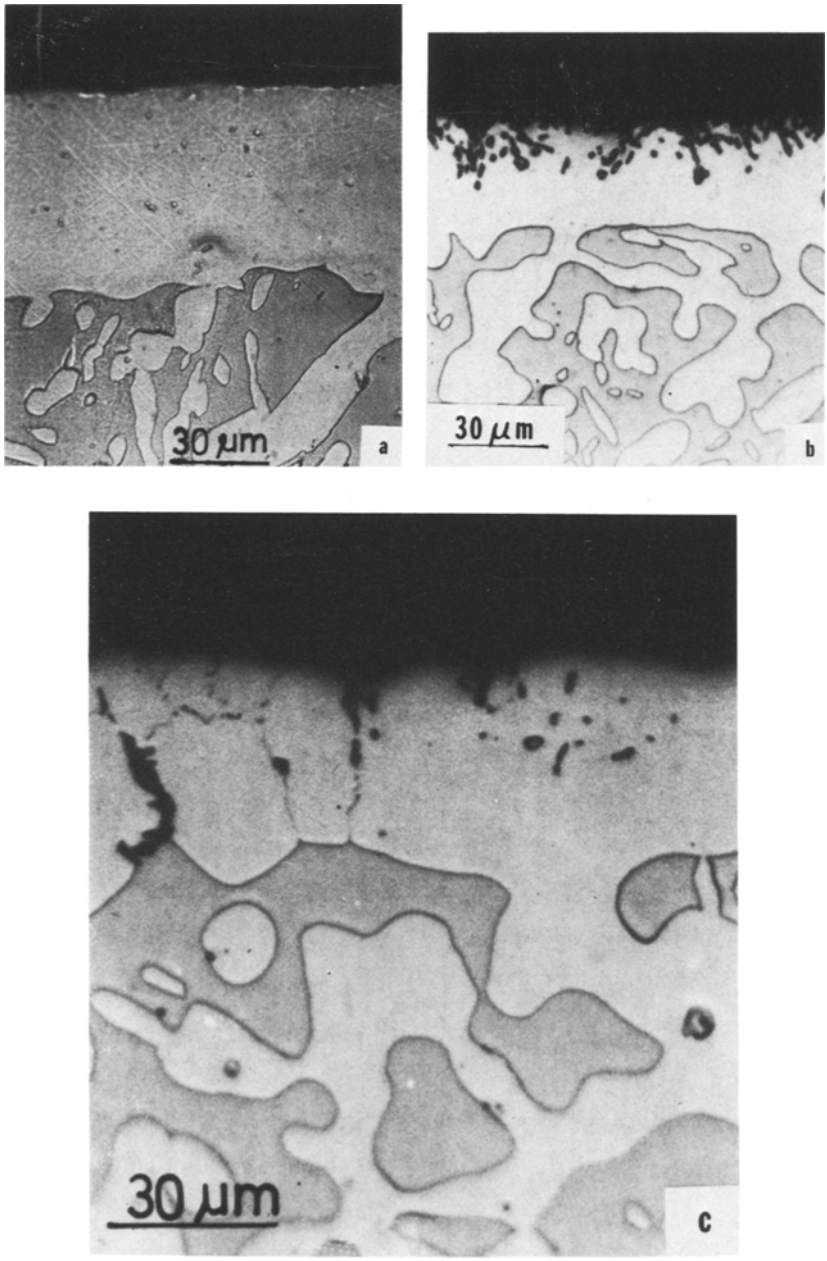

Fig. 2. Cross-sections of alloys oxidized at 1200°C for 50 hr: (a) CoCrAl; (b) CoCrAl-Hf; (c) CoCrAl-Y.

error in both of these numbers is certainly not less than ±15%. Calculation is complicated a little in the case of the other two alloys because of the internal oxidation and the possibility of oxidation of the active elements. However, neglecting those effects, the weight gain should be approximately half of that for the ternary alloy and the external scale thickness ratio less than half because of the internal oxide.

Actual weight gains could be measured accurately only for the Hf-containing alloy: the value was 2.0 mg/cm^2, in excellent agreement with the above estimate. Some scale spalled from the Y-containing alloy, and part was ejected from the crucible and lost. The residual weight gain was 0.7 mg/cm^2. For the ternary alloy, no weight gain figure could be determined because of the extensive spalling and ejection of the oxide. However, from previous work,[9] it can be estimated that a factor of 2 in the isothermal weight gain is approximately correct.

Peg Morphologies

Figure 3 shows SEM pictures of the underside of the scale and the residual metal on deep-etched specimens. From these and from the cross-sections shown in Fig. 2, it can be seen that the oxide/metal interface is quite smooth for the ternary alloy; the pegs in the case of the Y-containing alloy appear principally at the α-grain boundaries, penetrating through the single-phase region, and the pegs in the Hf-containing alloy are irregular rods of the sort described by Allam *et al.*,[3] and in Fe-10Al-1Hf alloys by Hindam and Whittle.[11] The peg structure in the Y-containing alloy is unusual: Allam found pegs at grain boundaries, but they appeared to be low aspect-ratio rounded cylinders. Grain boundary sheets have been observed in PVD coatings,[12] where they appear to be related to "leaders," which could be regarded as extended phase boundaries. Interestingly, PVD Co-Cr-Al coatings do not appear to develop such a well-defined single-phase depleted layer, and do apparently form aluminum oxide along the interconnected phase boundaries. This may be related to the coating procedure.

Figure 4 shows the differences in the internal oxide structure on the Hf-containing and Y-containing alloys. These are different areas of a shallow taper section a few degrees away from the metal surface: in essence, each metallograph can be regarded as a composite of sections parallel to the surface at different depths. The Hf-containing alloy shows the almost circular cross-sections of the thin pegs extending into the single phase region, and no oxidation of the two-phase region. In contrast, the Y-containing alloy shows the extended films around the grains in the single-phase region, and the oxide at the α-β-phase boundaries in the two-phase region.

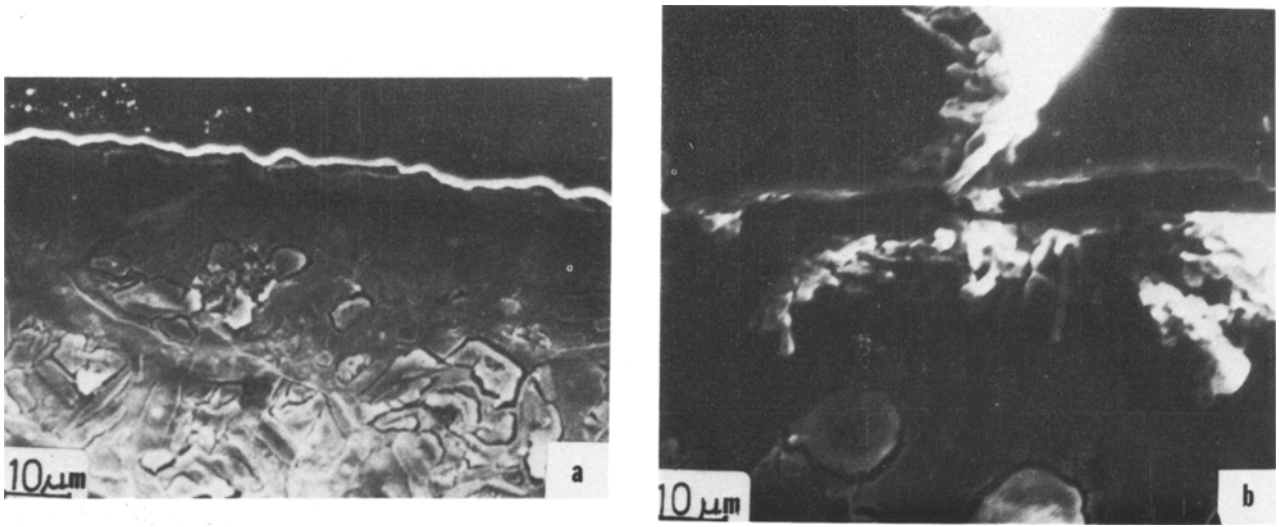

Fig. 3. SEM micrographs of oxidized alloys obtained by deep-etching. Oxidation at 1200°C for 50 hr. (a) CoCrAl; (b) CoCrAl-Hf; (c) CoCrAl-Y.

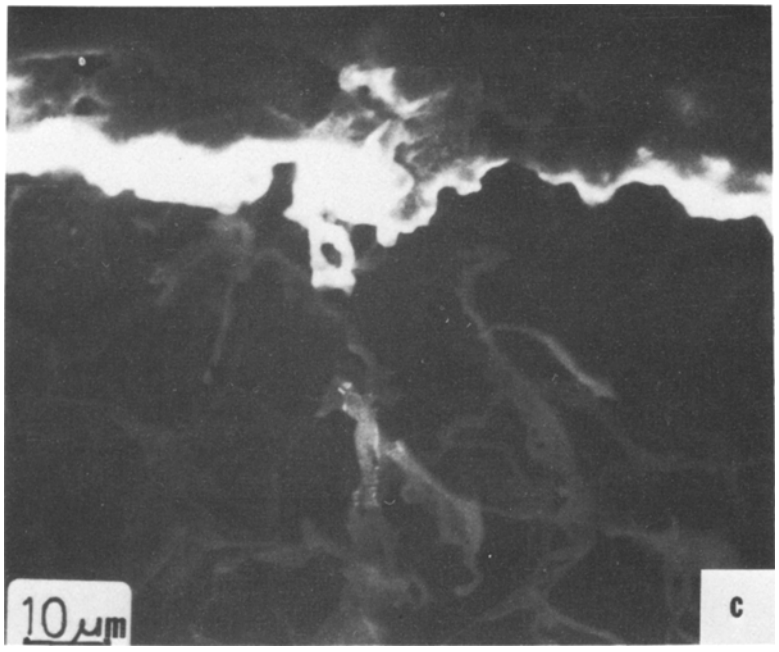

Fig. 3. Continued.

Figure 5 shows a deep-etched portion of Y-containing alloy. The light-colored features labeled (b) are the oxide sheaths at the boundaries; (a) is the metal. The EDXA of these two regions shows that the sheaths are very high in yttrium, presumably as Y_2O_3, and also contain Al, presumably as Al_2O_3. Morphologically, these appear to be films of Al_2O_3 encapsulating the Y_2O_3 formed by internal oxidation of the yttride phase.

DISCUSSION

The pegs formed in the Hf-containing alloy are consistent with earlier studies, and it is presumed that their growth depends either on short-circuit diffusion along the HfO_2/alloy boundaries, as proposed by Allam *et al.*,[3] or through HfO_2 particles in the external scale, effectively short-circuiting the scale.

In the case of the Y-containing alloy, although the pegs—or sheaths—do again mirror the internal phase distribution, the depth of penetration is remarkably great, up to 150 μm, and this implies an unreasonably high

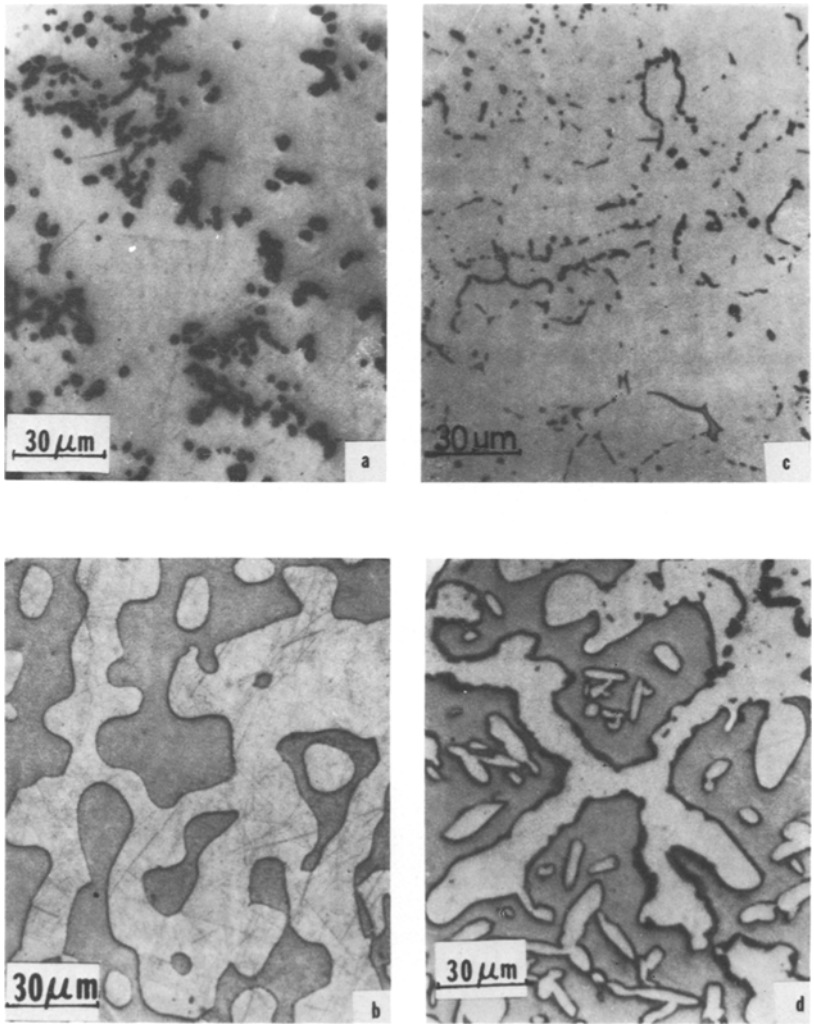

Fig. 4. Optical micrographs obtained by polishing shallow tapered sections, a few degrees from the oxidized surface. Oxidation at 1200°C for 50 hr. (a) CoCrAl-Hf, region in single phase zone close to oxide-alloy interface. (b) CoCrAl-Hf, region in two-phase zone a little away from oxide-alloy interface. (c, d) Same as in (a, b), respectively, but for CoCrAl-Y.

diffusion rate. This can be seen by calculating the depth of internal penetration expected using the model of Wagner.[14,15] If it is assumed that the thickness of the external scale is small compared to the depth of internal oxidation, and that the parabolic rate constant for internal oxidation is

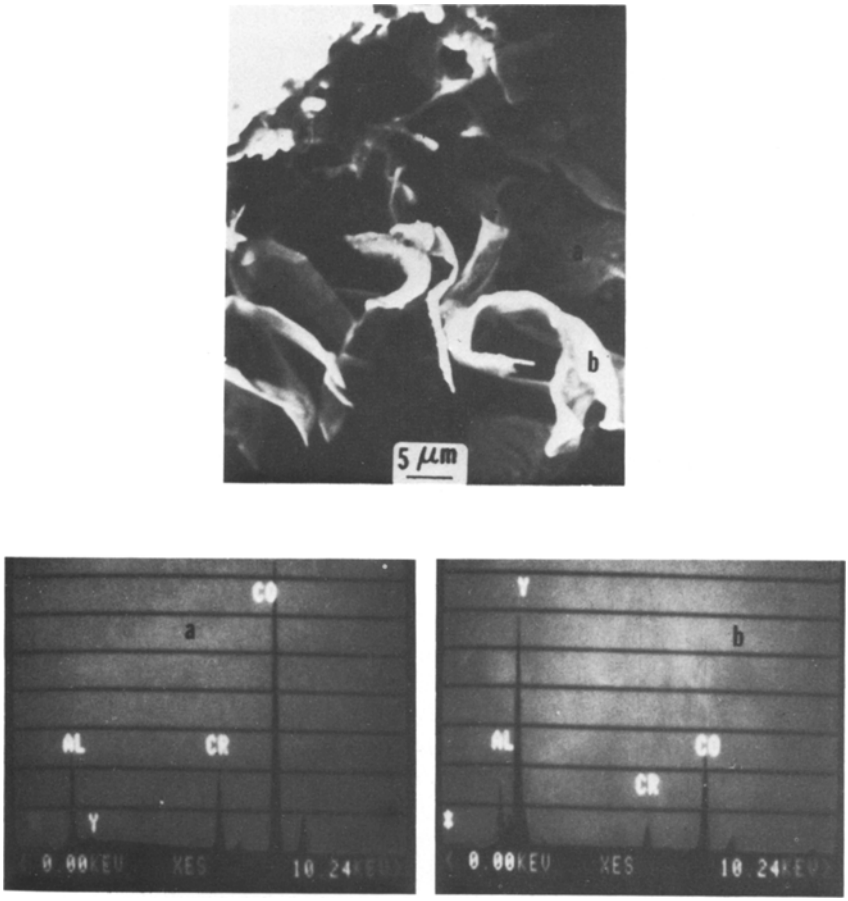

Fig. 5. Sheathlike morphology of internal oxides/pegs in oxidized CoCrAl-Y revealed by deep-etching as well as EDXA spectrum from the sheath and from the surrounding alloy. Labels "a" and "b" indicate precise regions from which the corresponding spectra were obtained.

small, Wagner's expression simplifies to

$$N_0^s D_0 = \frac{\nu N_{Al}(\xi - x)\xi}{2t} \cdot \frac{1}{F[\xi/2(D_{Al}t)^{1/2}]}$$

where N_{Al} is the bulk mole fraction of aluminum in the alloy; N_0^s is the oxygen solubility at the scale/alloy interface; D_0, D_{Al} are the diffusion coefficients of oxygen and aluminum in the alloy, respectively; x is the thickness of the scale; ξ is the depth of internal oxidation, measured from

the original metal surface; ν is the relative atomic concentration of oxygen in the oxide (=3/2 for Al_2O_3); and $F(u)$ is the auxiliary function, defined as $F(u)=\sqrt{\pi}u\exp(u^2)\operatorname{erfc}(u)$, where $\operatorname{erfc}(u)$ is the complementary error function. Further, by letting $x \ll \xi$ and $D_{Al} \ll D_0$, which appears to be valid in the present case, Eq. (1) further simplifies to

$$N_0^s \cdot D_0 = \frac{3N_{Al}\xi^2}{4t}$$

Now, setting $t=180$ ks, $N_{Al}=0.05$, and $\xi=10^{-4}$ m, then $N_0^s D_0 = 0.93\times10^{-15}$ m^2/s.

From internal oxidation studies on dilute cobalt-silicon alloys, Grundy and Nolan[15] give D_0 at 1200°C as approximately 2×10^{-11} m^2/s, from which

$$N_0^s = 0.47\times10^{-4}$$

This value is not intrinsically unlikely, since Seybolt[16] reports the solubility of oxygen in nickel with an extrapolated value at 1200°C of 4.3×10^{-4}. For Ni-Al, Whittle *et al.*[17] show that from a number of sources, N_0D_0 at 1200°C lies in the range

$$5\times10^{-14}-1\times10^{-12}\ \text{m}^2/\text{s}$$

Thus D_0 is in the range 1×10^{-11} to 2×10^{-8} m^2/s, rather higher than that for cobalt (although this is consistent with the internal oxidation results). However, these data relate to relatively dilute alloys (up to 4 wt.% Al) when the external oxide was NiO. Smeltzer and Whittle[18] have discussed the situation where the external and internal oxides were the same; the concentration of the solute element in the internally oxidized zone can then be significantly greater and the major driving force for the diffusion is the gradient of the aluminum rather than the gradient of oxygen. It might be expected in the present situation that D_0 would be greater and N_0^s less than for the dilute alloy situation.

For the Hf-containing alloy, the depth of the internal oxidation layer is only 10^{-5} m, and thus,

$$N_0^s \cdot D_0 \sim 10^{-17}\ \text{m}^2/\text{s}$$

It is difficult to see how the presence of the minor reactive element could significantly affect either D_0 or N_0. Whittle *et al.*[17] suggest that a difference in the permeability between Ni-Cr and Ni-Al alloys could be attributed to the fact that the internal oxide in the former case was in the form of unconnected particles, whereas in the latter case it was present as an interconnected network, and that phase boundary diffusion was responsible for the difference. However, the apparent enhancement decreased with increasing temperature, and should be fairly small at 1200°C.

For these reasons, it is postulated that the rapid ingress of oxygen is by a gaseous transport process through interconnected porosity along the internal oxide network. Although some porosity could be seen in both the optical and scanning electron micrographs, it is not possible to determine whether it is interconnected. Furthermore, it is well-known that porosity can be an artefact of specimen preparation. To test the hypothesis, therefore, a "reoxidation experiment" was performed.

Yttrium-containing specimens were oxidized in the normal way, and the surface was polished to remove the oxide, the single-phase depleted zone, and some part of the two-phase region. The polished specimens were then reoxidized. The oxidation was catastrophic, with considerable oxide formation and oxide penetration into the structure, as shown in Fig. 6. In contrast, Hf-containing specimens treated in the same way reoxidized in essentially the same manner as the fresh specimen, as shown in Fig. 7. This implies that in the case of the yttrium-containing alloys, paths allowing the rapid ingress of oxygen were present in the two-phase layer well in advance of the oxidation front and that these paths were developed by the initial oxidation; it seems difficult to believe that these were other than pores or channels at the phase boundaries. In contrast, no such channels were formed in the Hf-containing alloys.

Statements concerning the mechanism of formation of these channels must be purely speculative. One possibility is that the significant volume

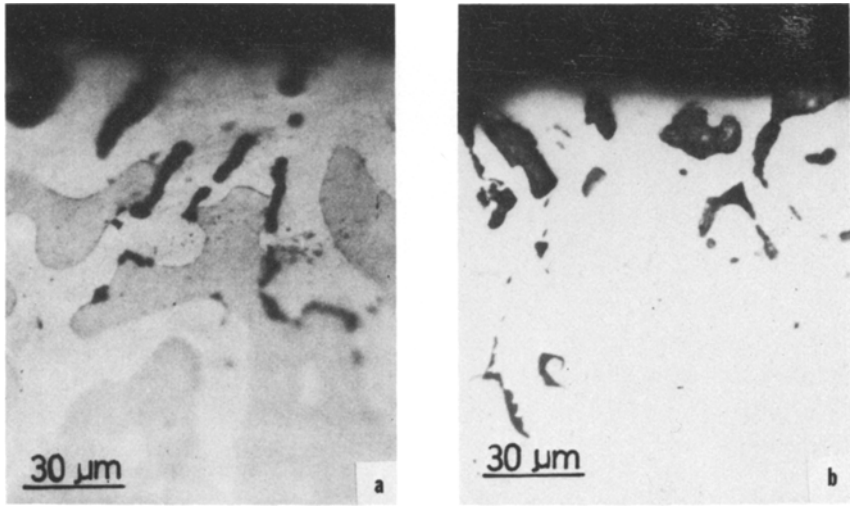

Fig. 6. (a, b) Typical cross-section micrographs of "reoxidized" (i.e., oxidized, polished, and oxidized again; see text) CoCrAl-Y. Catastrophic oxidation is evident.

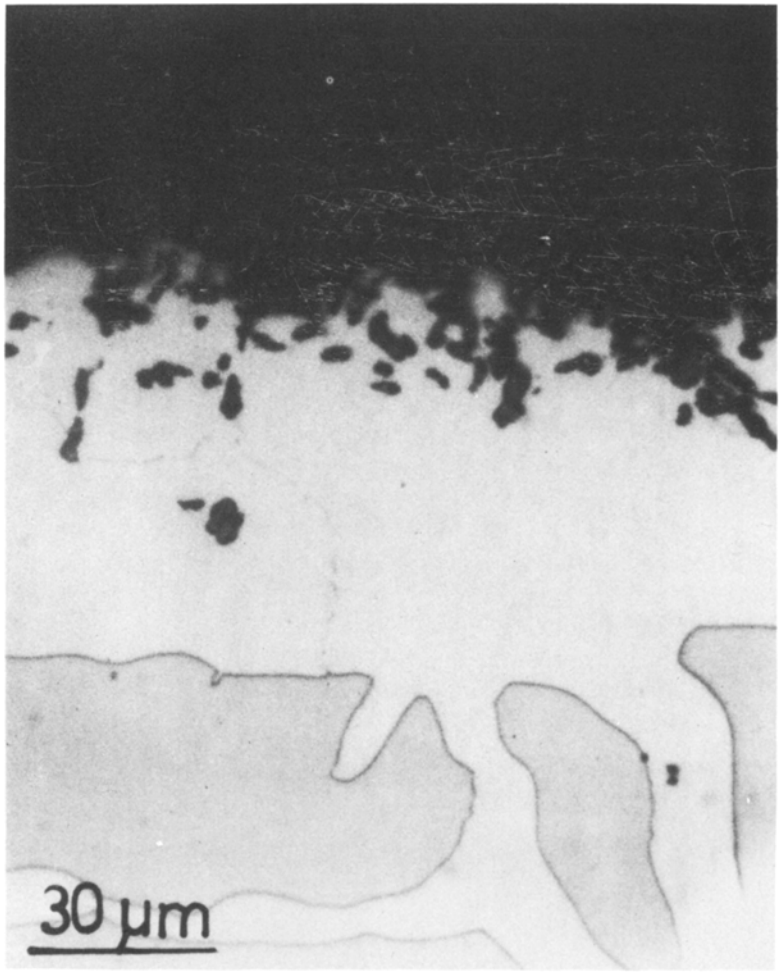

Fig. 7. Cross-section micrograph of "reoxidized" CoCrAl-Hf.

increase associated with the oxidation of the phase-boundary yttride particles induces cracking at the α-β phase boundaries (the Pilling-Bedworth ratio for yttrium oxidizing to Y_2O_3 is 1.133). Even if no actual cracking occurs, the large stresses may facilitate the rapid inward migration of oxygen.

It is well known that Co-Cr-Al-Y PVD coatings can suffer severe internal oxidation, and this is often associated with coatings which have "leaders," defects extending considerable distances through the coating. The possibility of the generation of channels by the internal oxidation of

yttrium could account for this behavior, and also explain why coatings treated so that the long-range interconnection of the two phases is eliminated have greatly improved oxidation resistance. The hafnium, since it is not present as a phase-boundary phase, could not be expected to generate phase-boundary channels.

CONCLUSIONS

The inward penetration of oxide into alumina-forming alloys containing reactive elements is usually believed to be beneficial, improving the adhesion of the external protective oxide scale. This is termed "pegging." However, deep internal oxide penetrations will not be beneficial. The can act as crack initiators at the oxide–metal interface, and can eventually lead to penetration of relatively thin protective coatings.

The depth of penetration appears to be related to the microstructure of the alloy. Where the reactive element is present as a distinct phase at the α-β phase boundaries in Co–Cr–Al base alloys, deep oxide penetrations along the phase boundaries may develop during high-temperature oxidation. Where the reactive element is in solid solution in the alloy, no such deep penetration is observed.

It is proposed that the oxygen penetrates into the alloy along channels at the phase boundaries, and that these channels are developed by the oxidation process itself. The most likely mechanism for their formation is cracking at the phase boundaries as a result of stresses developed due to the volume expansion associated with the oxidation of the reactive element-containing phase at the alloy phase boundaries. This degradation process can be avoided by (a) using a reactive element that does not form a distinct phase at the alloy phase boundaries, or (b) ensuring that the alloy phase boundaries do not form interconnected paths.

ACKNOWLEDGMENTS

The authors deeply acknowledge the invaluable guidance and criticism of the late Professor David P. Whittle during the course of this work. The work was supported by the Director, Office of Energy Research, Office of Basic Energy Sciences, Materials Sciences Division of the U.S. Department of Energy under Contract Number De-AC03-76SF00098.

REFERENCES

1. D. P. Whittle and J. Stringer, *Philos. Trans. R. Soc.* (London), **A295**, 309–329 (1980).
2. C. S. Giggins and F. S. Pettit, *Met. Trans.*, **2**, 1071–1078 (1971).

3. I. M. Allam, D. P. Whittle, and J. Stringer, *Oxid. Met.*, **12**, 35 (1978).
4. I. M. Allam, D. P. Whittle, and J. Stringer, *Oxid. Met.* **13**, 381 (1979).
5. J. Stringer, D. P. Whittle, and I. M. Allam, *Thin Solid Films* **45**, 377–384 (1977).
6. L. Kingsley, M. S. thesis, University of California, Berkeley (LBL Rep. No. 10952), April 1980.
7. I. M. Allam, H. C. Akuezue, and D. P. Whittle, *Oxid. Met.* **14**(6), 517–530 (1980).
8. D. P. Whittle, D. H. Boone, and I. M. Allam, *Thin Solid Films* **73**, 359 (1980).
9. I. M. Allam, PhD thesis, University of Liverpool, U.K. (1978).
10. J. Stringer, B. A. Wilcox, and R. I. Jaffee, *Oxid. Met.* **5**, 11–47 (1972).
11. H. Hindam and D. P. Whittle, *J. Electrochem. Soc.* **129**(5), 1147–1150 (1982).
12. S. J. Shaffer, D. H. Boone, and R. T. Lambertson, *Thin Solid Films* **107**, 463–472 (1983).
13. C. Wagner, *J. Electrochem. Soc.* **106**(8), 777 (1959).
14. C. Wagner, *Corr. Sci.* **8**, 889–893 (1968).
15. P. J. Grundy and P. Nolan, *J. Mat. Sci.* **7**(9), 1086–1087 (1972).
16. A. U. Seybolt, dissertation, Yale University, quoted in *Metals Reference Book*, 5th ed., C. J. Smithells, ed. (Butterworth, London, 1976).
17. D. P. Whittle, Y. Shida, G. C. Wood, F. H. Stott, and B. D. Bastow, *Philos. Mag. A*, **46**(6), 934–939 (1982).
18. W. W. Smeltzer and D. P. Whittle, *J. Electrochem. Soc.* **125**, 1116–1126 (1978).